Inductance calculations of permanent-magnet synchronous machines including flux change and self- and cross-saturations

Inductance Calculations of Permanent-Magnet Synchronous Machines Including Flux Change and Self- and Cross-Saturations

K. J. Meessen[1], P. Thelin[2], J. Soulard[3], and E. A. Lomonova[1]

[1]Department of Electrical Engineering, Eindhoven University of Technology, Eindhoven 5600 MB, The Netherlands
[2]SJ AB, Rolling stock division, Stockholm SE-105 50, Sweden
[3]Department of Electrical Machines and Power Electronics, School of Electrical Engineering, Royal Institute of Technology (KTH), Stockholm SE-100 44, Sweden

Accurate inductance calculation of permanent-magnet synchronous machines is a relevant topic, since the inductances determine a large part of the electrical machine behavior. However, the inductance calculation, as well as the inductance measurement, is never a completely straightforward task when saturation occurs. In this paper, the total flux in the d and q axes are obtained from finite-element method or measurements and therefore include saturation and cross-couplings. The inductances are obtained from analytical post-processing based on an equivalent magnetic circuit. The originality of this method is that it accommodates the changes in the magnet flux and the inductances with the level of saturation. The resulting inductance values are the ones seen by the converter or the grid, as found by a more accurate approach.

Index Terms—**Cross saturation, FEM, inductance calculation, permanent-magnet synchronous machine.**

I. Introduction

ACCURATE inductance calculation of permanent-magnet synchronous machines (PMSMs) is a relevant topic since the direct and quadrature (d and q) inductances determine a part of the torque, namely the reluctance torque, and the required terminal voltage of a converter-fed PMSM [1], [2]. For a line-start (direct-start) PMSM the d and q inductances also have an influence on the, e.g., obtained load angles for different torques, and to some extent also affect the starting possibilities. As pointed out in [3], wrong values of the inductances can lead to significant errors when predicting the motor performance.

Nevertheless, the inductance calculation, as well as the inductance measurement, is never a completely straightforward task. Numerous papers have been written and published on this subject, but all of the found papers seem to solve the problem by considering a constant magnet flux and taking the effect of saturation and cross-coupling in the d and q inductance values. Among numerous literature, it was found that [4] gives a good overview of the subject and presents briefly some different methods for inductance calculation, e.g., using the stored magnetic energy, the magnetic vector potential, or the air-gap flux density. The latter method, which is commonly used, excludes the slot leakage but it can be calculated quite accurately by analytical means.

As [5] correctly points out, it is not easy to determine a correct value of the d inductance (or d reactance) when the machine is saturated since the induced voltage, from the permanent-magnet flux, changes too. Therefore, [5] suggests the use of the Flux-MMF diagram, which is general for all electrical machines, when calculating the torque of the machine. This is a good suggestion but it does not improve the calculation of the d and q inductances that are required in the so commonly used dq phasor diagram. To solve this issue, [4] proposes the use of "frozen" permeabilities of the magnetic circuit in the finite-element method (FEM) calculations of inductance.

A different approach to the same problem is given in [6]. The use of iterative calculations is suggested when making a small angle displacement of the current in the measurement.

Reference [7] emphasizes the importance of using the fundamental values from a fast Fourier transform (FFT) of the voltages and currents when calculating the inductances to avoid the influence of slot harmonics, etc. This reflection is also shared by the authors of the present paper.

For inductance measurements, different methods are also proposed, such as a dc decay test, a static inductance bridge [3], or based on the flux linkage obtained from measurement of the phase voltage [7], [8]. For measurements, the rotor position is either measured with some kind of shaft position sensor, or an iterative calculation procedure as in [3] is used, but it is even possible to measure inductance without iterative calculations using only a conventional electrical power analyzer (i.e., without a direct measurement of the shaft position) as described in [9].

For analytical calculations, using lumped circuit models, imply approximations since the magnetic saturation behavior of all flux paths in the iron laminations seldom are easy to pinpoint exactly. Lumped circuit models in combination with iterative calculations, as well as the FEM calculations, can easily cope with the magnetic saturations in the different parts of the magnetic circuit, but even though such phenomena are considered the calculations of the d and q inductances seen by the converter or the grid can be troublesome. The reasons for this can still be said to be due to the nonlinear behavior of the iron laminations. This nonlinear behavior has the ability to "hide" the wanted inductances even if the FEM calculations are used since it is not obvious to determine how much flux is produced solely by a positive d current when the magnetic saturation occurs. The problem occurs with desaturation for a negative d current as well. Cross-saturation, i.e., the saturation of iron parts in one direction due to flux from current in the other direction (and vice versa), also complicates the determination of the produced flux.

Digital Object Identifier 10.1109/TMAG.2008.2001419

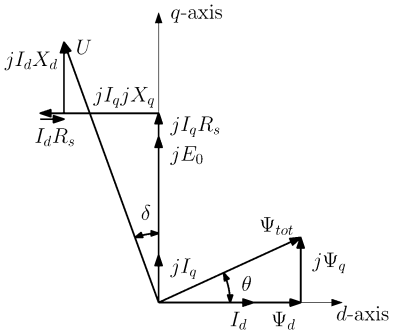

Fig. 1. Conventional dq phasor diagram for winding voltage, current, and flux linkage in a PMSM.

By using the theory of magnetic equivalent circuits (MEC) [10], (Section III), and even introducing diodes in the derived equivalent circuit, (Section IV), this paper derives and presents some simple and easy-to-use analytical equations for the calculation of the d and q inductances and corrected induced voltage using the induced voltages obtained from FEM or measurements. By using results from FEM calculations or measurements, it is possible to include the effects of both changing permanent-magnet flux, and self- and cross-saturation in the d and q inductance calculations. The obtained values for the inductances are therefore the values seen by the converter or the grid. The presented method is original in the way that it considers that the magnet flux is depending on the level of saturation. Our method is therefore similar to the one presented in [11] in the way that it post-processes FEM results. However, in [11] it is assumed that the magnet flux does not depend on the level of saturation and is therefore considered constant.

Since the calculation method derived in the present paper is a post-processing one that can be applied to both calculated and measured flux linkages, it is not possible to verify the accuracy of this method by measurements. However, the obtained results can be analyzed and compared to the conventional method which assumes constant magnet flux.

II. Conventional Inductance Calculations of a PMSM

In a permanent-magnet synchronous machine, the relation between the current and voltage can be described by

$$U = jE_0 + I_dR_s + jI_dX_d + jI_qR_s + j(jI_q)X_q \quad (1)$$

where U is the winding voltage phasor, E_0 is the no-load voltage phasor produced by the permanent magnets only, assumed to be constant at a given speed and a constant temperature, and R_s is the winding resistance. I_d and I_q are the winding current phasors and X_d and X_q are the reactances in the d and q direction, respectively. The graphical representation of (1) is shown in Fig. 1 in the form of a phasor diagram, where Ψ_d, Ψ_q, and $\Psi_{\rm tot}$ are the flux linkages seen by the windings [12], [13].

From Fig. 1, with current applied only in the d direction (I_d current), and with $\omega L = X$, the inductance L_d can be defined as

$$L_d = \frac{\sqrt{U^2 - (R_sI_d)^2} - E_0}{\omega I_d} \ (\text{for } I_q = 0). \quad (2)$$

When current is applied only in the q direction (I_q current), the inductance L_q can be defined as

$$L_q = \frac{\sqrt{U^2 - (E_0 + R_sI_q)^2}}{\omega I_q} \ (\text{for } I_d = 0). \quad (3)$$

The electrical quantities in (2) and (3) are obtained either from measurements or FEM calculations. Both cross-saturation and the change of the permanent-magnet flux due to saturation are neglected in (2) and (3). In the following sections, a method to include these phenomena is presented.

III. Inductance Calculations With Varying Permanent-Magnet Flux

A. Magnet-Flux Change for I_d or I_q Current

In both (2) and (3), the no-load voltage, E_0, is assumed to be constant for a given speed during operation and it is calculated at no-load conditions. The value of the no-load voltage E_0 depends on the flux produced by the magnet in the air gap, Φ_m, the speed of the rotor, and the winding configuration. The flux, Φ_m, is defined as the value of the magnetomotive force (MMF) source representing the magnet, divided by the total *nonlinear* reluctance, $\mathcal{R}_d$, in the d direction, which includes the air-gap reluctance, $\mathcal{R}_g$, the internal magnet reluctance, $\mathcal{R}_m$, and the nonlinear iron reluctance, $\mathcal{R}_i$. Since the flux produced by the stator current, Φ_I, saturates or desaturates the iron, the nonlinear reluctance, $\mathcal{R}_i$, changes when a current is applied. Therefore, assuming a constant E_0 during operation is only valid when the armature flux in the air gap, Φ_I, is small compared to Φ_m or, when the working point of the magnetic circuit is below the knee of the B–H curve of the iron-lamination in the machine, i.e., where $\mathcal{R}_i$ is assumed to be constant.

Assuming now that $\mathcal{R}_i$ depends on the current, E_0, X_d, and X_q become functions of the currents I_q and I_d. The changed values of no-load voltage, E_0, and the flux linkage in the d-axis, Ψ_d, when only I_q is applied, are easy to obtain from Fig. 1. The values of U, δ, $\Psi_{\rm tot}$, and θ are calculated from FEM results, and R_s and I_q are known. Now, the changed or compensated no-load voltage is

$$E_{0,\rm comp} = U\cos(\delta) - R_sI_q \quad (\text{for } I_d = 0). \quad (4)$$

The compensated no-load voltage has now possibly a value different from the no-load value, E_0, due to saturation. And the flux linkage due to the permanent magnet is obtained by

$$\Psi_m = k_1\Phi_m = \Psi_d = \Psi_{\rm tot}\cos(\theta) \quad (\text{for } I_d = 0) \quad (5)$$

where Ψ_m and Φ_m are the flux linkage and flux produced by the permanent magnet only, respectively, and k_1 is a constant. By combining (3) and (4), the q inductance, when taking into account the change of E_0 due to q current, is

$$L_q = \frac{U\sin(\delta)}{\omega I_q} \quad (\text{for } I_d = 0). \quad (6)$$

Because the flux linkage due to d current in the air gap, Ψ_{Id}, has the same or the opposite direction as the magnet flux linkage

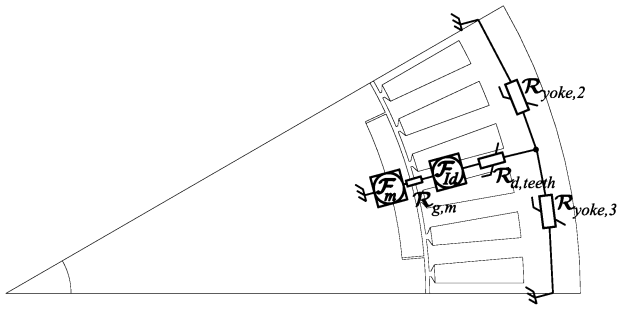

Fig. 2. Magnetic equivalent circuit for the d flux, here drawn in an inset permanent-magnet machine layout.

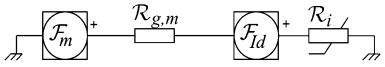

Fig. 3. Magnetic equivalent circuit for the d current.

Ψ_m, it is not possible to separate them. Therefore, it has traditionally been assumed that the no-load voltage, E_0, is constant, and that the saturation is all accounted for in the varying L_d.

Starting from the magnetic equivalent circuit in the d direction of the machine, shown in Fig. 2, a different way to separate Ψ_{Id} from the total d flux linkage, Ψ_d, is found and presented here. Fig. 2 shows the magnetic equivalent circuit for the flux in the d direction. $\mathcal{R}_{\mathrm{yoke},2}$ and $\mathcal{R}_{\mathrm{yoke},3}$ represent the nonlinear iron yoke reluctances (the rotor and stator yoke reluctances are merged), $\mathcal{R}_{d,\mathrm{teeth}}$ is the nonlinear teeth reluctance, and $\mathcal{R}_{g,m}$ is the sum of the air-gap reluctance and the internal magnet reluctance. $\mathcal{F}_m$ is the MMF source representing the magnet, and $\mathcal{F}_{Id}$ is the MMF source representing I_d. The value of $\mathcal{F}_m$ can be found by

$$\mathcal{F}_m = \frac{B_r l_m}{\mu_0 \mu_m} \tag{7}$$

where B_r is the remanent flux density of the permanent magnet at the actual permanent-magnet temperature, l_m is the radial thickness of the permanent magnet, μ_0 is the permeability of vacuum, and μ_m is the relative permeability of the permanent magnet. The value of $\mathcal{F}_{Id}$ is

$$\mathcal{F}_{Id} = \frac{3\sqrt{2}}{\pi} k_p k_s k_d q n_s I_d \tag{8}$$

where k_p is the pitch factor, k_s is the skewing factor, k_d is the distribution factor, q is the number of stator slots per pole per phase, and n_s is the number of stator winding turns per slot [14]. An alternative to (8) is to derive a constant $k_2 (\mathcal{F}_{Id} = k_2 I_d)$ by increasing the current in a FEM calculation until the same value for the fundamental of the air-gap flux density as produced by the magnets is obtained. When this flux density occurs, $\mathcal{F}_{Id} = \mathcal{F}_m$ as given by (7).

From the circuit drawn in the machine layout in Fig. 2, a simpler circuit can be made. In Fig. 3, the nonlinear reluctances $\mathcal{R}_{d,\mathrm{teeth}}$, $\mathcal{R}_{\mathrm{yoke},2}$, and $\mathcal{R}_{\mathrm{yoke},3}$ of Fig. 2 are combined into one nonlinear reluctance $\mathcal{R}_i$.

As the circuit is nonlinear, superposition cannot be applied; however, $\mathcal{R}_i$ increases for higher flux and the following relation for the total flux in the d direction can be stated

$$\Phi_{d,\mathrm{tot}} \leq \Phi_{m,Id=0} + \Phi_{Id,m=0} \quad (\text{for } \mathcal{F}_{Id} \geq 0). \tag{9}$$

Nevertheless, for $\mathcal{F}_{Id}$ or $\mathcal{F}_m$ equal to zero, the following two decompositions can be made:

$$\Phi_m = \frac{\mathcal{F}_m}{\mathcal{R}_{g,m} + \mathcal{R}_i(\Phi_m)} \quad (\text{for } \mathcal{F}_{Id} = 0) \tag{10}$$

$$\Phi_{Id} = \frac{\mathcal{F}_{Id}}{\mathcal{R}_{g,m} + \mathcal{R}_i(\Phi_{Id})} \quad (\text{for } \mathcal{F}_m = 0). \tag{11}$$

When both MMF sources, $\mathcal{F}_m$ and $\mathcal{F}_{Id}$, are not equal to zero, the total flux, $\Phi_{d,\mathrm{tot}}$, is

$$\Phi_{d,\mathrm{tot}} = \frac{\mathcal{F}_m + \mathcal{F}_{Id}}{\mathcal{R}_{g,m} + \mathcal{R}_i(\Phi_{\mathrm{tot}})}. \tag{12}$$

From this equation, it follows that the part of the total d flux that is produced by the magnet is

$$\Phi_{d,\mathrm{tot},m} = \frac{\mathcal{F}_m}{\mathcal{R}_{g,m} + \mathcal{R}_i(\Phi_{\mathrm{tot}})}. \tag{13}$$

Combining (12) and (13) gives the part of the total flux produced by the magnet

$$\begin{aligned} \Phi_{d,\mathrm{tot},m} &= \Phi_{d,\mathrm{tot}} \frac{\mathcal{F}_m}{\mathcal{F}_m + \mathcal{F}_{Id}} \\ &\propto \Psi_{d,\mathrm{tot}} \frac{\mathcal{F}_m}{\mathcal{F}_m + \mathcal{F}_{Id}} = \Psi_{\mathrm{tot}} \cos(\theta) \frac{\mathcal{F}_m}{\mathcal{F}_m + \mathcal{F}_{Id}}. \end{aligned} \tag{14}$$

Since the no-load voltage is a linear function of the air-gap flux linkage due to the permanent magnets, the value of the compensated no-load voltage, $E_{0,\mathrm{comp}}$, can be calculated from the FEM results. With only d current applied to the windings of the machine and replacing Ψ_{tot} by U, and θ by δ in (14)

$$E_{0,\mathrm{comp}} = U \cos(\delta) \frac{\mathcal{F}_m}{\mathcal{F}_m + \mathcal{F}_{Id}} \tag{15}$$

and a rewritten (2) in combination with (15) yield

$$\begin{aligned} L_d &= \frac{U \cos(\delta) - E_{0,\mathrm{comp}}}{\omega I_d} \\ &= \frac{U \cos(\delta)}{\omega I_d} \frac{\mathcal{F}_{Id}}{\mathcal{F}_m + \mathcal{F}_{Id}} \quad (\text{for } I_q = 0) \end{aligned} \tag{16}$$

where (16) gives an expression for the d inductance including the changing flux of the permanent magnets due to saturation effects. Basically, it has been derived that the new proposed method splits the effect of saturation on both the magnet flux and the armature flux in proportion to the respective magnet and current MMF.

IV. Inductance Calculation Including Cross-Saturation Effects

In the previous section, a method to calculate the values of L_d and L_q inductances is given for only d or q current applied to the windings. In practice, most machines are controlled by applying both d and $q$currents at the same time. In this situation, the L_d

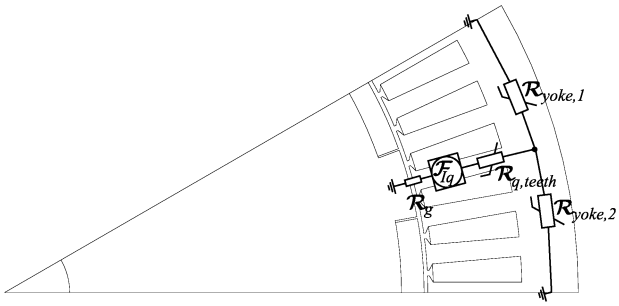

Fig. 4. Magnetic equivalent circuit for the I_q current flux, drawn in an inset permanent-magnet machine layout.

and L_q inductances change due to so-called cross-saturation. This cross-saturation occurs because the flux in the q direction and the flux in the d direction share partly the same magnetic path.

A. L_q Inductance

From the phasor diagram in Fig. 1, it follows that the L_q inductance again can be directly calculated with the load angle, δ, and the winding voltage, U, and the resistive voltage drop due to the d current, $R_s I_d$. Therefore, when I_d and I_q are applied at the same time, the L_q inductance is defined by

$$L_q = \frac{U \sin(\delta) + I_d R_s}{\omega I_q}. \tag{17}$$

B. L_d Inductance

For calculation of the L_d inductance when both I_d and I_q are applied, the same problem as in the previous section arises. To calculate the d inductance, the value of E_0 is necessary. But now, the real value of E_0 during operation is affected by saturation due to both d-flux and q-flux components.

To find a better expression for the d inductance, a new magnetic equivalent circuit for both d flux and q flux is derived. The new magnetic equivalent circuit is a combination of the magnetic equivalent circuit for d flux shown in Fig. 2 and the magnetic equivalent circuit for q flux shown in Fig. 4. The magnetic equivalent circuit for q flux shown in Fig. 4 has a lot of similarities with the magnetic equivalent circuit for d flux in Fig. 2. The circuit consists of a constant air-gap reluctance, $\mathcal{R}_g$, the MMF source, $\mathcal{F}_{Iq}$, represents the q current, and the nonlinear iron reluctances, $\mathcal{R}_{q,\mathrm{teeth}}$, $\mathcal{R}_{\mathrm{yoke},1}$, and $\mathcal{R}_{\mathrm{yoke},2}$. The value of $\mathcal{F}_{Iq}$ can be found from (8), by simply replacing I_d by I_q. Combining the two magnetic equivalent circuits results in the magnetic equivalent circuit presented in Fig. 5.

As can be seen in Fig. 5, the flux produced by the magnet and the d current (d flux) share only the yoke-reluctances with the q flux. That simplification has been done since the main parts of the air gap d and q fluxes flow in different teeth. Mostly, this simplification will only have a small impact on the final result. This is more true when the magnet width is less than 180 electrical degrees (in the considered motor the magnets cover 120 degrees of the pole) and when the flux waveform from the current is more sinusoidal. The common rotor yoke (core) reluctance has not been neglected, but it is now for simplification merged with the nonlinear stator yoke reluctance in Figs. 5 and 6. Two separate grounds in the circuit of Fig. 5 are introduced because the ground defines a point of symmetry that is different for the d and q flux paths. To avoid confusion, the q flux and the d flux conductors are drawn as two different lines which are connected to the yoke reluctances.

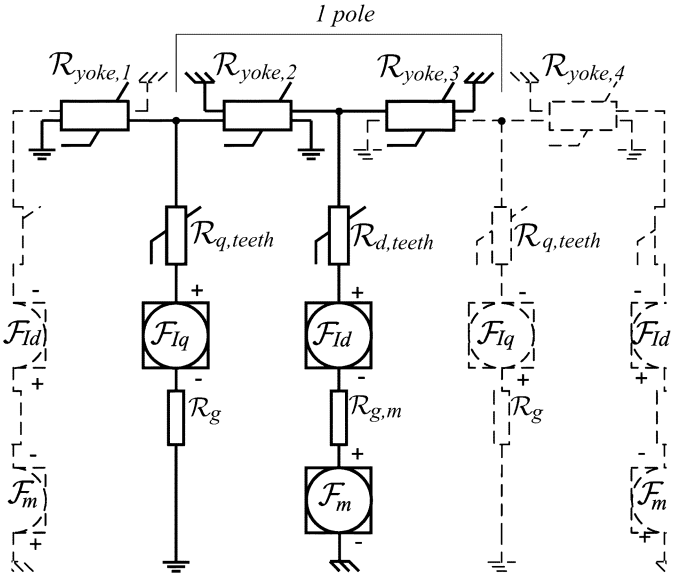

Fig. 5. Magnetic equivalent circuit with both d current and q current.

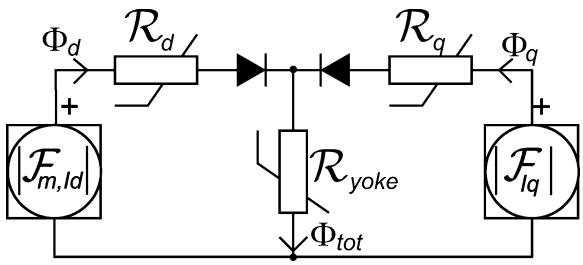

Fig. 6. Magnetic equivalent circuit for the both d and q currents.

When both I_d and I_q are applied, the total flux distribution is not symmetric along the d and q axes, respectively. For example, when both $\mathcal{F}_{Iq}$ and $\mathcal{F}_{Id} + \mathcal{F}_m$ are positive, the d flux counteracts the q flux through $\mathcal{R}_{\mathrm{yoke},2}$ and thus, the resulting flux through $\mathcal{R}_{\mathrm{yoke},2}$ is lowered. At the same time, the d flux and q flux have the same direction through $\mathcal{R}_{\mathrm{yoke},3}$ and therefore, the resulting flux through $\mathcal{R}_{\mathrm{yoke},3}$ is higher than the resulting flux through $\mathcal{R}_{\mathrm{yoke},2}$. All the yoke reluctances are functions of the flux through them. Therefore, when both d and q fluxes are in the magnetic equivalent circuit

$$\mathcal{R}_{\mathrm{yoke},1} \neq \mathcal{R}_{\mathrm{yoke},2} \tag{18}$$

$$\mathcal{R}_{\mathrm{yoke},3} \neq \mathcal{R}_{\mathrm{yoke},4} \tag{19}$$

$$\mathcal{R}_{\mathrm{yoke},2} \neq \mathcal{R}_{\mathrm{yoke},3} \tag{20}$$

$$\mathcal{R}_{\mathrm{yoke},1} \neq \mathcal{R}_{\mathrm{yoke},4}. \tag{21}$$

The amount of flux produced by $\mathcal{F}_{Iq}$ in the positive q axis direction, is the same as the amount of flux produced by $\mathcal{F}_{Iq}$ in the negative q axis direction, only the sign is opposite. The same holds for the flux produced by $\mathcal{F}_{Id}+\mathcal{F}_m$. Since it is not possible for the main part of the q flux to go through the d axis teeth

reluctances and vice versa, and due to the geometric symmetry of the electrical machine, it can be stated that

$$\mathcal{R}_{\mathrm{yoke},2}//\mathcal{R}_{\mathrm{yoke},3} = \mathcal{R}_{\mathrm{yoke},1}//\mathcal{R}_{\mathrm{yoke},4} \tag{22}$$

and

$$\mathcal{R}_{\mathrm{yoke},1}//\mathcal{R}_{\mathrm{yoke},2} = \mathcal{R}_{\mathrm{yoke},3}//\mathcal{R}_{\mathrm{yoke},4} \tag{23}$$

even when there are both d and q fluxes in the electrical machine. The sign $//$ is used to signify parallel connection which means that $A//B = (AB)/(A+B)$. As the machine is odd-symmetric with a period of one pole

$$\mathcal{R}_{\mathrm{yoke},3} = \mathcal{R}_{\mathrm{yoke},1} \tag{24}$$

and

$$\mathcal{R}_{\mathrm{yoke},2} = \mathcal{R}_{\mathrm{yoke},4}. \tag{25}$$

Combining (24) and (25) with (22) and (23) gives

$$\begin{aligned} &\mathcal{R}_{\mathrm{yoke},2}//\mathcal{R}_{\mathrm{yoke},3} \\ &= \mathcal{R}_{\mathrm{yoke},1}//\mathcal{R}_{\mathrm{yoke},4} \\ &= \mathcal{R}_{\mathrm{yoke},1}//\mathcal{R}_{\mathrm{yoke},2} \\ &= \mathcal{R}_{\mathrm{yoke},3}//\mathcal{R}_{\mathrm{yoke},4}. \end{aligned} \tag{26}$$

This means that the nonlinear yoke reluctance for the q flux, which is the parallel connection of $\mathcal{R}_{\mathrm{yoke},1}$ and $\mathcal{R}_{\mathrm{yoke},2}$, is equal to the nonlinear yoke reluctance of the d flux, which is the parallel connection of $\mathcal{R}_{\mathrm{yoke},2}$ and $\mathcal{R}_{\mathrm{yoke},3}$. From this conclusion, the equivalent circuit in Fig. 5 can be redrawn as the magnetic equivalent circuit for the absolute values of the fluxes presented in Fig. 6.

In Fig. 6, the nonlinear reluctance, $\mathcal{R}_d$, consists of the air-gap reluctance, $\mathcal{R}_g$, the internal magnet reluctance, $\mathcal{R}_m$, and the nonlinear teeth reluctance for the d flux $\mathcal{R}_{d,\mathrm{teeth}}$. $\mathcal{R}_q$ is nonlinear too and consists of the air-gap reluctance, $\mathcal{R}_g$, and the nonlinear teeth reluctance for the q flux $\mathcal{R}_{q,\mathrm{teeth}}$. $\mathcal{R}_{\mathrm{yoke}}$ is the common yoke reluctance for the d flux and the q flux.

Because the q flux cannot use the d flux teeth path and vice versa, two ideal diodes had to be introduced in the circuit to make it valid. As the diodes block negative q flux and negative d flux as well, a problem arises when a negative current is applied. Therefore, the q flux source in the circuit is set to the absolute value of $\mathcal{F}_{Iq}$. This is valid because of the symmetry of the q flux path: a negative $\mathcal{F}_{Iq}$ in Fig. 5 results in an exchange of $\mathcal{R}_{\mathrm{yoke},1}$ with $\mathcal{R}_{\mathrm{yoke},4}$ and $\mathcal{R}_{\mathrm{yoke},2}$ with $\mathcal{R}_{\mathrm{yoke},3}$. Therefore, the circuit in Fig. 6 is still valid when a negative q current is applied.

$\mathcal{F}_m$ and $\mathcal{F}_{Id}$ are series-connected in the same flux path. Therefore, they can be replaced by one MMF source, $\mathcal{F}_{m,Id}$. This source has the same symmetry properties as $\mathcal{F}_{Iq}$, see above. So, in the circuit in Fig. 6, the MMF sources, $\mathcal{F}_m$ and $\mathcal{F}_{Id}$, are replaced by the absolute value of the sum of them both, $|\mathcal{F}_{m,Id}| = |\mathcal{F}_m + \mathcal{F}_{Id}|$.

Since the reluctances in Fig. 6 are nonlinear, superposition cannot be applied. For the absolute values of only permanent-magnet flux, only d current flux or only q current flux the following three decompositions can be stated

$$\Phi_m = \frac{\mathcal{F}_m}{\mathcal{R}_d(\Phi_m) + \mathcal{R}_{\mathrm{yoke}}(\Phi_m)} \quad (\mathcal{F}_{Id} = 0, \mathcal{F}_{Iq} = 0) \tag{27}$$

$$\Phi_{Id} = \frac{|\mathcal{F}_{Id}|}{\mathcal{R}_d(\Phi_{Id}) + \mathcal{R}_{\mathrm{yoke}}(\Phi_{Id})} \quad (\mathcal{F}_m = 0, \mathcal{F}_{Iq} = 0) \tag{28}$$

$$\Phi_{Iq} = \frac{|\mathcal{F}_{Iq}|}{\mathcal{R}_q(\Phi_{Iq}) + \mathcal{R}_{\mathrm{yoke}}(\Phi_{Iq})} \quad (\mathcal{F}_m = 0, \mathcal{F}_{Id} = 0). \tag{29}$$

When all the MMF sources produce flux, the total flux is equal to or lower than the sum of the fluxes in (27)–(29) because of the nonlinearity of the iron. The total flux can be defined by a part of the flux in the d direction, and a part of the flux in the q direction

$$\Phi_{\mathrm{tot}} = \underbrace{\frac{|\mathcal{F}_m + \mathcal{F}_{Id}|}{\mathcal{R}_d(\Phi_d) + \mathcal{R}_{\mathrm{yoke}}(\Phi_{\mathrm{tot}})}}_{d-\mathrm{flux},\Phi_d} + \underbrace{\frac{|\mathcal{F}_{Iq}|}{\mathcal{R}_q(\Phi_q) + \mathcal{R}_{\mathrm{yoke}}(\Phi_{\mathrm{tot}})}}_{q-\mathrm{flux},\Phi_q}. \tag{30}$$

Combining (30) with information from Fig. 1 gives that the absolute value of the d flux is proportional to

$$\Phi_d = \frac{|\mathcal{F}_m + \mathcal{F}_{Id}|}{\mathcal{R}_d(\Phi_d) + \mathcal{R}_{\mathrm{yoke}}(\Phi_{\mathrm{tot}})} \propto |\Psi_{\mathrm{tot}} \cos\theta|. \tag{31}$$

Since $\mathcal{F}_m + \mathcal{F}_{Id}$ and $\cos\theta$ always have the same sign, the absolute signs in (31) can be removed. Equation (31) looks similar to (12) and by splitting in the same way the d flux in a part produced by the magnet and a part produced by the d current, the flux produced by the magnet is proportional to

$$\begin{aligned} \Phi_{\mathrm{tot},m} &= \frac{\mathcal{F}_m}{\mathcal{R}(\Phi_d) + \mathcal{R}_{\mathrm{yoke}}(\Phi_{\mathrm{tot}})} \\ &\propto \Psi_{\mathrm{tot}} \cos(\theta) \frac{\mathcal{F}_m}{\mathcal{F}_m + \mathcal{F}_{Id}}. \end{aligned} \tag{32}$$

This can be interpreted as the varying value of E_0 by replacing the total flux linkage Ψ_{tot} by U and the angle θ by δ, and subtracting the resistive voltage drop

$$E_{0,\mathrm{comp}} = (U\cos(\delta) - R_s I_q) \frac{\mathcal{F}_m}{\mathcal{F}_m + \mathcal{F}_{Id}}. \tag{33}$$

The value of $E_{0,\mathrm{comp}}$ is not equal to the no-load voltage E_0 due to the saturation of the iron by d current flux, q current flux, and the magnet flux. With this compensated value of E_0 from (33), it is possible to give an expression for the d inductance, L_d, when both d and q current are applied to the machine at the same time

$$\begin{aligned} L_d &= \frac{U\cos(\delta) - R_s I_q - E_{0,\mathrm{comp}}}{\omega I_d} \\ &= \frac{U\cos(\delta) - R_s I_q}{\omega I_d} \frac{\mathcal{F}_{Id}}{\mathcal{F}_m + \mathcal{F}_{Id}}. \end{aligned} \tag{34}$$

In most machines, the resistive voltage drop, $R_s I_q$, in (34) is very small compared to the winding voltage U at relatively high speeds, and may be neglected.

TABLE I
SPECIFICATIONS PMSM

Property	Value	Description
N_p	12	Number of poles
n	1500	Base speed
-	AI1010	Laminated steel type
t	0.35 mm	Lamination thickness
B_r	1.2 T	Remanent flux density permanent magnets

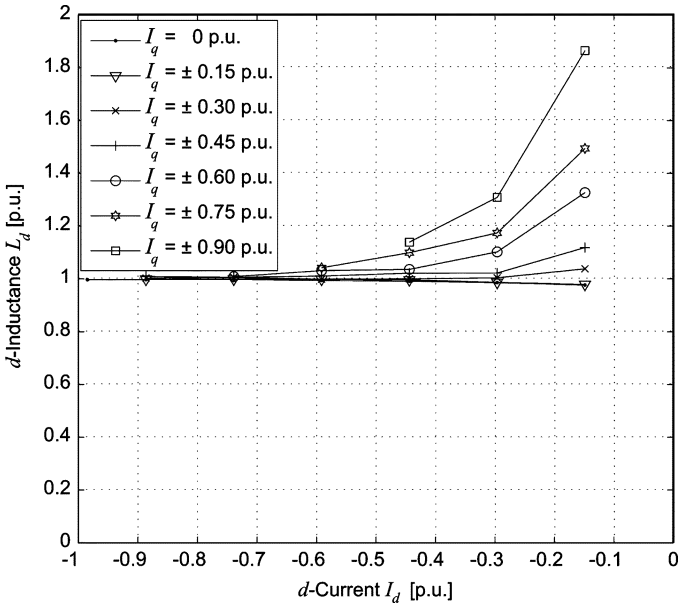

Fig. 7. d inductance versus negative d current for several values of q current, calculated assuming constant magnet flux.

V. SIMULATION RESULTS

The method for calculating inductances described previously is applied to data obtained from FEM calculations on a PMSM by using commercially available software [15]. The modeled machine is a conventional PMSM with inset mounted permanent magnets as described in Table I and shown in Fig. 2. In this section, the results of the simulations are presented.

The FEM simulations are performed on a twelve-pole permanent-magnet synchronous machine. The values of the flux density in the air-gap and the winding voltage are obtained by time-stepping simulations, made for one electrical period with the machine running at constant speed. First, simulations are done for only d current and only q current. In the simulations for only d current, the q flux is zero, and the d flux consists of magnet produced flux and d current produced flux. In the simulations with only q current, the d current is zero and the d flux is equal to the magnet produced flux.

Considering no cross-saturation, and calculating the inductance by using (34) with E_0 instead of $E_{0,\mathrm{comp}}$ results in the d inductances shown in Fig. 7. The d inductance increases rapidly for high values of q current. This is completely opposite to what is expected due to cross-saturation, and caused by the assumption that E_0 is constant.

A. Change of Flux Produced by the Permanent Magnets

Fig. 8 shows the peak value of the fundamental of the air-gap flux density produced by the permanent magnets for different current values. The flux density is calculated from FEM results using (5) and (14). As can be seen from Fig. 8, the air-gap flux density produced by the permanent magnets decreases up to 15% for positive d current, while it even slightly increases for low negative d current values and is constant for high negative d current. Because both magnet flux and flux produced by positive d current have the same direction, the positive d current increases the level of saturation of the iron in the teeth and in the yoke. The higher level of saturation results in a higher equivalent reluctance value. Therefore, the magnet flux decreases for positive d current.

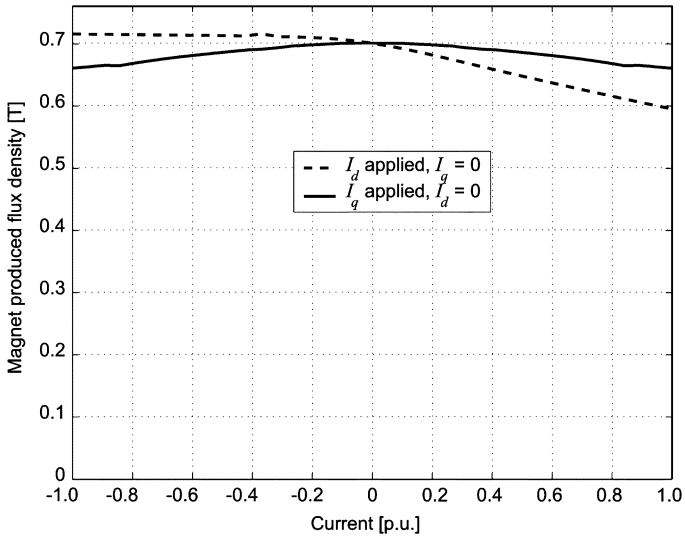

Fig. 8. Changed peak value of the magnet produced flux density in the air gap for different currents. The dotted line shows the change of magnet produced flux density due to saturation by current applied in the d direction, the solid line shows the effect of current applied in the q direction.

On the other hand, negative d current lowers the level of saturation as the flux produced by the negative d current opposes the magnet produced flux. Fig. 8 shows an almost constant flux density for negative d current. This occurs because the negative d current sets the flux density level to the linear part of the B–H curve of the iron, i.e., below the knee of the B–H curve.

Contrary to flux produced by d current, q flux shares only part of its path (the stator and rotor yokes) with the magnet flux path. Therefore, saturation due to q current has less influence on the magnet produced flux. Flux from both negative and positive q current components saturates a part of the permanent-magnet flux path as can be seen in Figs. 5 and 6. Therefore, Fig. 8 shows symmetric behavior for positive and negative q current.

B. Results of Inductance Calculations

With (17) and (34), the values of the d and q inductances are calculated from FEM results. Because of the magnetic symmetry in the q direction of the machine, the direction of the q current does not influence the inductance values. Therefore, all simulations are only performed for positive q current while the results are valid for positive and negative q current. All presented values have been normalized by dividing the calculated inductance by the d inductance found for the rated current of the machine.

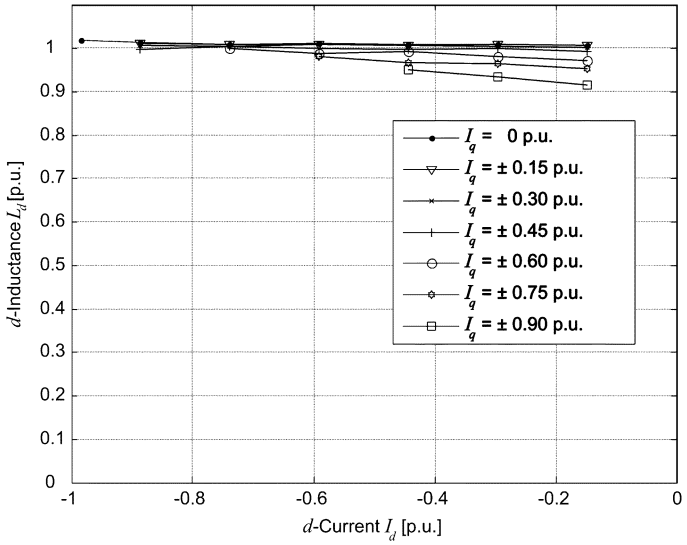

Fig. 9. d inductance versus **negative *d* current** for several values of q current. Calculated using the winding voltage from FEM results.

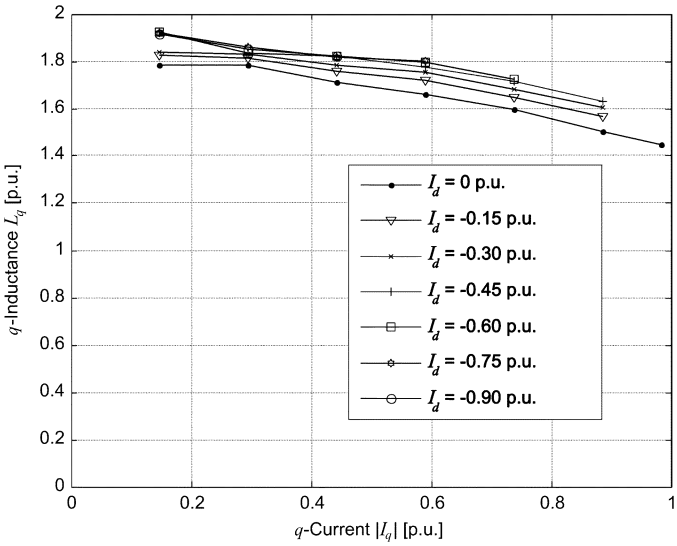

Fig. 11. q inductance versus the absolute value of q current for several values of **negative *d* current**. Calculated using the winding voltage from FEM results.

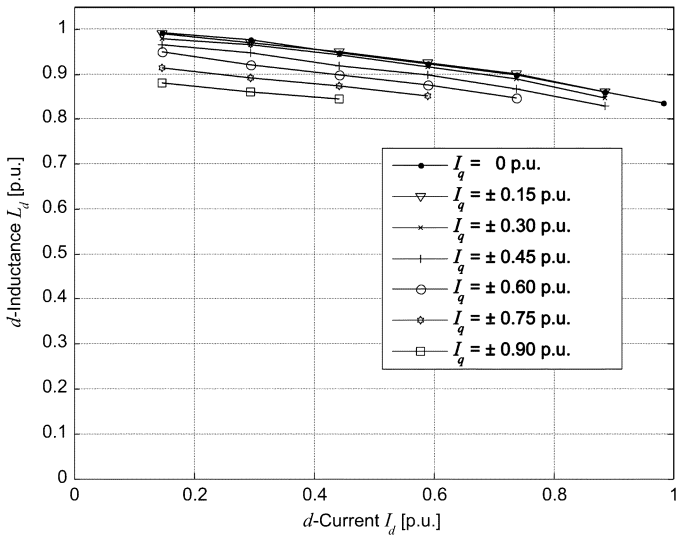

Fig. 10. d inductance versus **positive *d* current** for several values of q current. Calculated using the winding voltage from FEM results.

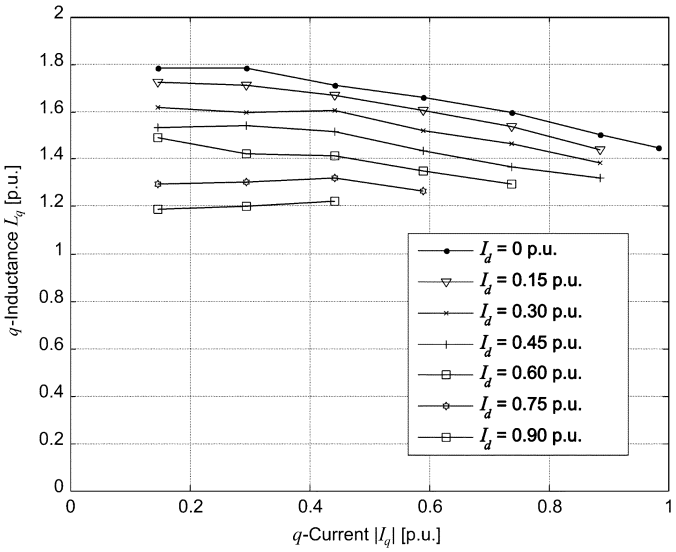

Fig. 12. q inductance versus the absolute value of q current for several values of **positive *d* current**. Calculated using the winding voltage from FEM results.

1) L_d Inductance: Fig. 9 shows values of the d inductance versus negative d current for different values of q current. As can be seen in the figure, the d inductance is almost constant when no I_q is applied. This agrees with the results from Fig. 8. The permanent magnet produced flux does not increase when a negative d current is applied. So, the reluctance value of the iron is constant in this region. This results in a constant inductance value.

When a higher value of I_q is applied as well, the iron saturates and the d inductance decreases. For higher values of negative d current, the d inductance increases because the negative d current opposes the permanent magnet produced flux and the iron will desaturate.

In Fig. 10, the d inductance versus positive d current for different values of q current is plotted. The iron saturates more for higher values of d current because the flux produced by the d current has the same direction as the flux produced by the permanent magnet. Therefore, the inductance value decreases for higher values of d current. As the flux produced by the q current shares partly the same path as the d flux, the iron goes even deeper into saturation when q current is applied as well. Therefore, the value of the inductance lowers even more when both q current and positive d current are applied.

2) L_q Inductance: The results for the q inductance show similar behavior as the results for the d inductance. Fig. 11 shows the q inductance versus the absolute value of the q current for different values of negative d current. The inductance decreases for higher values of q current due to saturation of the iron. When negative d current is applied at the same time, the inductance increases due to the desaturation effect of the negative d current. Fig. 12 shows the q inductance versus the absolute value of q current for different positive values of d current. The positive d

current produces more flux in the d direction. Therefore, the iron already saturated by q current flux, goes deeper into saturation by the positive d current flux since it adds to the flux from the permanent magnet. This results in a lower value of q inductance when positive d current is applied.

The slightly increasing q inductance at a d current of 0.75 and 0.9 p.u. is probably caused by numerical calculation errors. A very small deviation in the angle δ causes a significant deviation in the inductance value in this region.

VI. Conclusion

This paper has presented four analytical equations, (6), (16), (17), and (34), which can easily be used in combination with FEM calculations or measurements to obtain the d and q inductances values of a permanent-magnet synchronous machine taking into account saturation and cross-couplings. This implies that the obtained inductance values include the effects of both self- and cross-saturations as well as the change of permanent-magnet flux due to magnetic saturation of the iron parts of the machine. The equations are derived by using the theory of magnetic equivalent circuits in combination with symmetrical and nonsymmetrical conditions of the electrical machine magnetic circuit. The derived equations have been applied to the results from FEM calculations on a permanent-magnet synchronous machine design and the obtained d and q inductances values versus applied d and q currents show behavior that follows the laws of electromagnetics in nonlinear materials, which was not the case assuming a constant permanent-magnet flux.

References

[1] Y. S. Chen, Z. Q. Zhu, and D. Howe, "Calculation of d- and q-axis inductances of PM brushless ac machines accounting for skew," *IEEE Trans. Magn.*, vol. 41, no. 10, pp. 3940–3942, Oct. 2005.

[2] R. Dutta and M. F. Rahman, "A comparative analysis of two test methods of measuring d- and q-axes inductances of interior permanent-magnet machine," *IEEE Trans. Magn.*, vol. 42, no. 11, pp. 3712–3718, Nov. 2006.

[3] P. Mellor, F. Chaaban, and K. Binns, "Estimation of parameters and performance of rare-earth permanent-magnet motors avoiding measurement of load angle," *IEE Proc. B, Elect. Power Appl.*, vol. 138, pp. 322–330, Nov. 1991.

[4] N. Bianchi and S. Bolognani, "Magnetic models of saturated interior permanent magnet motors based on finite element analysis," in *Proc. Industry Applications Conf*, Oct. 1998, vol. 1, pp. 27–34.

[5] T. Miller, M. Popescu, C. Cossar, M. McGilp, and J. Walker, "Calculating the interior permanent-magnet motor," in *Proc. IEEE Int. Electric Machines and Drives Conf.*, Jun. 2003, vol. 2, pp. 1181–1187.

[6] B. Stumberger, B. Kreca, and B. Hribernik, "Determination of parameters of synchronous motor with permanent magnets from measurement of load conditions," in *Proc. IEEE Int. Electric Machines and Drives Conf.*, Dec. 1999, vol. 14, pp. 1413–1416.

[7] K. Rahman and S. Hiti, "Identification of machine parameters of a synchronous motor," *IEEE Trans. Ind. Appl.*, vol. 41, no. 2, pp. 557–565, Mar./Apr. 2005.

[8] B. Stumberger, G. Stumberger, D. Dolinar, A. Hamler, and M. Trlep, "Evaluation of saturation and cross-magnetization effects in interior permanent-magnet synchronous motor," *IEEE Tran. Ind. Appl.*, vol. 39, no. 5, pp. 1264–1271, Sep./Oct. 2003.

[9] H. Nee, L. Lefevre, P. Thelin, and J. Soulard, "Determination of d- and q-reactances of permanent-magnet synchronous motors without measurements of the rotor position," *IEEE Trans. Ind. Appl.*, vol. 36, no. 5, pp. 1330–1335, Sep./Oct. 2000.

[10] G. R. Slemon, *Electric Machines and Drives.*. Reading, MA: Addison-Wesley, 1992.

[11] L. Chédot and G. Friedrich, "A cross saturation model for interior permanent magnet synchronous machine. application to a starter-generator," in *Proc. IEEE Industry Applications Conf.*, Oct. 2004, vol. 1, pp. 64–70.

[12] L. Serrano-Iribarnegaray, "The modern space-phasor theory, part I: Its coherent formulation and its advantages for transient analysis of converted-fed ac machines," *Eur. Trans. Elect. Power Eng., ETEP*, vol. 3, pp. 171–180, Mar. 1993.

[13] L. Serrano-Iribarnegaray, "The modern space-phasor theory, part II: Comparison with the generalized machine theory and the space-vector theory," *Eur. Trans. Elect. Power Eng., ETEP*, vol. 3, pp. 213–219, May 1993.

[14] C. Sadarangani, *Electrical Machines—Design and Analysis of Induction and Permanent Magnet Motors.*. Stockholm, Sweden: Royal Institute of Technology, 2000.

[15] CEDRAT, "FLUX2D version 9.3.1.," CAD Package for Electromagnetic and Thermal Analysis Using Finite Elements..

Manuscript received December 4, 2007; revised June 11, 2008. Current version published September 19, 2008. Corresponding author: K. Meessen (e-mail: kmeessen@ieee.org).